Journal of Materials Chemistry B

Accepted Manuscript

ROYAL SOCIETY OF CHEMISTRY

www.rsc.org/materialsB

Title: Fabrication of a novel blended membrane with chitosan and silk microfibers for wound healing: characterization, *in vitro* and *in vivo* studies

Authors: Zongpu Xu[†], Liyang Shi[†], Mingying Yang, Haiping Zhang, Liangjun Zhu[*]

Institute of Applied Bioresource Research, College of Animal Science, Zhejiang University, Hangzhou 310058, PR China

[*]**Corresponding author:** Liangjun Zhu, Prof. Ph.D., College of Animal Science, Zhejiang University

Tel.: +86 0571 88982185; fax: +86 0571 88982185

Email address: ljzhu@zju.edu.cn (L.Zhu).

Postal address: Room C319, Agriculture Life and Environmental Sciences Building, Institute of Applied Bioresource Research, College of Animal Science, Zhejiang University, 866 Yuhangtang Road, Hangzhou, 310058, Zhejiang Province, PR China

Abstract

Pure chitosan membranes present insufficient mechanical properties and high swelling ratio, which limited their application in biomedical field. In this study, silk microfibers were obtained by chemical hydrolysis and a novel type of chitosan/silk microfibers(CS/mSF) blended membranes were reported, following with multiple physical properties evaluated. Mechanical properties were significantly increased after blending silk microfibers with chitosan matrix, while swelling ratio decreased. Surface microstructures observation of blended membranes via scanning electron microscope showed abundant embedment of mSF into CS matrix, as well as connection among mSF. The cytocompatibility *in vitro* was also investigated, and blended membranes exhibited impressive cytocompatibility, which was demonstrated by cell proliferation and cell morphology. Furthermore, *in vivo* healing effects of blended membrane as a wound dressing was carried on full-thickness skin wound model of rats. Animal studies revealed that membranes containing mSF showed increased efficiency of wound healing compared with pure CS membranes and

non-wound dressing treatment. From histological changes examination, a higher level of epithelialization and collagen formation were observed under the treatment of CS/mSF blended membranes after 21-day repair period. In conclusion, our results indicated that the blended membranes with CS and mSF had great attraction as a potential candidate material for wound healing.

1. Introduction

Skin could be easily injured by different causes such as heat, mechanical force, physical and chemical agents, which lead to threat for human health. One of therapies used for accelerating skin regeneration and reducing scar formation is coverage of the damaged skin with wound dressing. [1] An ideal wound dressing material should not only act as a baffle wall against bacteria and dust, but also exhibit good biocompatibility, provide a moist and absorbing environment, as well as control gaseous permeation, etc.[2] Those derived from biological macromolecules gained more attention due to their biocompatibility, biodegradability and renewability.

Chitosan(CS) is a natural macromolecule linked through β-(1,4) glycosidic bonds between D-glucosamine and N-acetyl-D-glucosamine[3], which shows favorable biocompatibility, biodegradability, antibacterial property and wound healing effect. CS have currently been studied in tissue engineering, drug delivery, cancer diagnosis, especially wound healing.[4-6,7,8] However, pure CS materials present insufficient mechanical properties and high swelling ratio. To overcome these limitations, blending CS with other materials to fabricate different forms of wound dressings has become an important methodology.[9-12] Silk fibroin(SF) is a fascinating natural protein extracted from cocoons of *Bombyx mori* silkworm, due to its excellent mechanical properties,

great biocompatibility, controllable biodegradability and remarkable air permeability.[13-15] SF thus has been designed as materials for biomedical applications such as tissue engineering and drug delivery[16-19, 20], as well as wound repair.[21-23] In order to availably combine the advantages of CS and SF, previous studies have blended CS with SF solution or lyophilized SF solid to fabricate composite wound dressing materials.[10, 24-26] However, the mechanical properties, biological stability and durability of those blended materials performed not very well as wound dressings, otherwise crosslinker reagent may became a potential risk. On the other hand, the use of crosslinker reagent[3] or toxic organic solvents like HFIP and TFA during the electrospinning process[25, 26] may became a potential risk.

Silk microfibers(mSF) are prepared directly from degummed silk fibers, and have been used as reinforcement in three-dimensional matrix like hydrogels and scaffolds to obtain better mechanical and cellular outcomes.[27-30] Therefore, we hypothesized that a novel wound dressing material could be fabricated by blending CS with mSF, instead of SF solution or lyophilized SF solid. In the current study, different contents of mSF were introduced into CS matrix to prepare blended membranes and improve the properties of resulting membranes. Multiple physical properties of blended membranes including mechanical properties, thermal behaviors, swelling ratio and water vapor transmission rate were strictly investigated. Furthermore, *in vitro* cytocompatibility, and *in vivo* wound healing effects with or without mSF on the full-thickness skin wound model of rats were comprehensively evaluated. Through this work, we provide valuable insights into the role of mSF in membrane reinforcement, and illustrate the increased efficiency of wound healing effects of CS/mSF blended membranes compared to pure CS membranes from both macroscopy and microscopy.

2. Results and Discussion

2.1Morphology of mSF and membranes

mSF of different length could be obtained by controlling the duration of alkaline hydrolysis. According to SEM images, after hydrolyzing for 6 hours, the length of mSF was over 200μm with significant varieties(Fig.1A), while decreased to 50-200μm of relative homogeneity after 12 hours(Fig.1B), and particles with irregular sharp points instead of microfibers were developed after 24 hours(Fig. 1C). The alkaline hydrolysis process seemed slower and milder than that reported by Mandal et al [27], due to the much lower concentration of NaOH solution. As a reinforcement filler, mSF with different sizes would improve mechanical properties of the matrix, and here in order to fabricate uniform blended membranes and to further investigate the *in vitro* and *in vivo* studies, mSF of 50-200μm were selected. The photographs of membranes in wet condition and their surface microstructures were shown in Fig.2. Pure CS membrane and CS/mSF blended membranes with various mass ratios of mSF presented very different morphology in terms of color, transparency, and surface roughness. CS/mSF blended membranes presented milk white in color and relatively low transmittance compared with transparent pure CS membrane. Pure CS membrane was so supple to entirely unfold with pincette, but the rigidities increased after adding mSF. When the mass ratio was 40% mSF were dispersed and embed in the CS matrix, and different degrees of cross and overlap even winding among mSF could also be viewed when it came to 60% and 80%, which all resulted in the rough surface of CS/mSF blended membranes.

2.2 Mechanical properties of CS/mSF blended membranes

Mechanical properties play important roles in process of tissue regeneration and further clinical

application.[31] Stress-strain curves of pure CS and CS/mSF blended membranes in wet condition, together with their elastic modulus, tensile strength, and elongation at break were shown in Fig.3. Compared with pure CS membrane, elastic modulus and tensile strength of 40% CS/mSF blended membrane showed a little difference. With further addition of mSF, elastic modulus and tensile strength of 60% CS/mSF blended membrane significantly increased to 9.96±1.73MPa and 3.21±0.77Mpa, respectively, and more significantly were 20.43±2.58MPa and 3.89±0.71Mpa when mass ratio of mSF reached 80%. Elongation at break were also increased to different degrees after adding mSF.

Addition of inorganic fillers such as carbon nanotubes and hydroxyapatite have been reported to enhance mechanical properties of CS matrix materials [32, 33], but they are not biodegradable. Our results demonstrated that natural organic mSF acted effectively as reinforcement fillers to improve mechanical properties of such membranous biocomposites, so mSF may be a feasible alternative. In this study, mSF were dispersed with random orientation in CS matrix indicating anisotropic stress transmission when stretched, which led to no significant improvement of mechanical properties. Apart from mSF mass ratio, we considered mSF-CS matrix adhension or interfacial cohesion as a contributing factor, but it seemed not obvious in 40% CS/mSF blended membranes. More interesting thing was the fact that 60% and 80% CS/mSF blended membranes showed multifold improvement effect. We thought with increasing mSF content the fiber-fiber interaction including cross, overlap and winding strengthened, which needed more force to break. According to previous studies [28, 29], the biocomposite properties are influenced by the fiber content, fiber distribution and fiber-matrix adhension. Thus one plausible explanation was that improved mechanical properties were mainly attributed to the interaction among mSF, and partially to

mSF-CS matrix adhension.

2.3 Thermal behaviors of CS/mSF blended membranes

To evaluate thermal behaviors of membranes and provide information about interaction between CS and mSF, we carried out thermogravimetric analysis(TGA) and differential scanning calorimetry(DSC) analysis. TGA curves of pure CS and CS/mSF blended membranes were presented in Fig.4A. Two obvious transitions can be observed, the first is from 200℃ to 250℃ and the second around 340℃. By increasing mSF content, the thermal stability could be gradually enhanced. DSC curves were shown in Fig.4B, and the exothermic peak at 296℃ would be due to the thermal decomposition of amine units of CS.[34] As we know, the thermal decomposition temperature of silk is affected by structural and morphological properties, like different molecular conformations. The decomposition temperature of well-oriented silk fibers is above 300℃; β-sheet structure of silk fibers thermally degrades at 290-295℃; α-helix and random coil structure decompose below 290℃.[35] Blended membranes had an endothermic peak at approximately 322℃, so we deduced that mSF embedded in CS matrix were well-oriented. No significant difference was observed in decomposition temperatures of CS/mSF blended membranes with various ratios, indicating physical connections were formed between CS molecule and mSF fillers.

2.4 Swelling ratio and Water Vapor Transmission Rate(WVTR) of CS/mSF blended membranes

At the early stage of wound healing, a wound dressing material should be capable to absorb exudates released from wound region, and to prevent both excessive dehydration and buildup of exudates. We tested two relevant parameters, swelling ratio and WVTR. As shown in Fig.5, both swelling ratio and WVTR of blended membranes significantly decreased after incorporating mSF,

mainly due to the high hydrophobic crystalline structure of silk fibroin by reducing affinity between water molecular and membranes [36], thus further decreased water uptake and penetration rate. However, blended samples still exhibited high capibility to absorb water, and even 80% CS/mSF blended membrane attained 2.14±0.72 (g/g). It is reported that the WVTR of intact skin ranged from 240 to 1920 g/m^2 per 24 h while that of uncovered wound is in order of 4800 g/m^2 per 24h.[37] WVTR of tested membranes in this study varied from 1209.94 to 1569.66g/m^2 per 24h, similar to intact skin and far below blank group, which could not only avoid risk of wound dehydration but also provide a sufficient moist environment.

2.5 Cell proliferation and morphology

Nontoxicity and biocompatibility of biomaterials are necessary for the future clinical applications. Proliferation and morphology of L929 cells cultured onto pure CS membrane and CS/mSF blended membranes for 1 and 3 days were shown in Fig.6. L929 cells could be able to attach and spread on all types of membranes and the cell number increased gradually with culture duration, suggesting that blended membranes presented non-cytotoxicity and an ability to support cell proliferation. MTS assay revealed no significant difference between and pure CS membrane, neither a definite change rule among blended membranes with different mass ratios of mSF(Fig.6A). However, according to SEM images(Fig.6B), the morphology of L929 cells attached onto tested membranes at 3 days showed obvious distinctions. For CS/mSF blended membranes, the attached cells presented more typically elongated shape, and plentiful filopodia could be clearly observed, especially the mass ratio of mSF was 80%.

Substrate stiffness and surface topography of material can affect cells in multiple aspects, such as proliferation, migration and differentiation.[38-40] In this study, the embedded mSF in CS matrix

together with the connection among mSF such as cross and winding offered attachment and support for L929 cells. The filopodia was another proof for better morphology, indicating that L929 cells could migrate with the guidance of mSF. These results demonstrated that CS/mSF blended membranes exhibited good cytocompatibility, and 80% CS/mSF blended membrane could provide the best microenvironment for cell behaviors.

2.6 Wound healing effect

Based on the impressive performance of blended membranes, we further investigated wound healing effects of 80% CS/mSF blended membrane as a wound dressing on rats. Full-thickness skin wound models have been generally utilized to evaluate the wound healing effects of different types of wound dressings.[21, 41, 42] In this study, circular full-thickness wounds of 2cm in diameter were formed on the back of rats, and covered with pure CS membrane and 80% CS/mSF blended membrane, vaseline cream as a blank control. Representative photographs of wound healing at time point of 0, 7, 14, and 21 days after different treatments were shown in Fig.7, and histological changes of wound sections stained with H&E were shown in Fig.8. During repair period, the control group with non-wound dressing presented the biggest wound size, while the wound area under treatment of wound dressings significant closed, indicating an accelerated efficiency. After 7 days, wound areas in the control group increased to 124.68±7.79%, while wounds covered with pure CS membrane and CS/mSF blended membrane decreased to 54.66±9.22% and 40.73±8.6%, respectively(Fig.7B). After 14 days, wound area covered with CS/mSF blended membrane was similar to pure CS membrane, but at 21 days wound area covered with CS/mSF blended membrane was much smaller than CS pure membrane, almost totally closed.

Skin wound healing is a complicated process including various cells and growth factors, it roughly

involves four phases of hemostasis, inflammation, proliferation and remodeling.[43] Inflammation could be generated once the injury initiated, and intensified after foreign materials adhered to the wound. At 7 days, injured skin covered with pure CS membrane showed red color with a smooth outline on the contact interface, while the wound area treated by CS/mSF blended membrane were red brown and the outlines were clearly rough(Fig.7A). Silk fibroin has been recognized nontoxic and less inflammatory [44, 45], but tissue edema was seen around parts of the wounds in CS/mSF blended membrane group(Fig.7A). This may be in consequence of mixed mediums, for pure CS membrane was a smooth single-phase system while CS/mSF blended membrane was a rough two-phase system. As a result, the inflammation process would be more intense and time-consuming, which could be reflected by the inflammatory cells appearing in large quantities mainly distributed on the border of wound and biomaterials at 7 days(Fig.8). From histology observation, granulation tissue also emerged in wound dressing treatment groups, but the amount was much more in CS/mSF blended membrane group. At 14 days, the wound color tended to thin and inflammatory cells were significantly decreased. Many new blood vessels could be seen in all groups, which were essential for the continued process. At 21 days, the newly-generated skin had the similar color with normal skin and blood vessels decreased, while it seemed no obvious change in control group. One notable difference was that hair follicle cells could be observed in CS/mSF blended membrane group(Fig.7A). The fibroblasts uniformly distributed in better order, and the collagen deposition was considerable. indicated partial recovery of normal structure and function.

Chitosan could activate macrophages, thus help fibroblasts proliferation and collagen synthesis[46], and this promoted emergence and maturation of granulation tissue. Silk fibroin has been

confirmed to boost epithelization in several studies.[2, 31, 47, 48] We deduced that with continuous epithelization, CS and mSF showed a synergistic effect. To summarize, we firmly believed that CS/mSF blended membrane achieved the best healing efficiency, as the macroscopy level of wound size was the smallest and the microscopy level of tissue was completely repaired. Therefore, Silk microfibers embedded in CS matrix improved wound healing at both macroscopy and microscopy levels. There is also a need to evaluate other relevant indexes to explain and charify the detail in wound healing.

3. Conclusion

Diverse length of mSF could be obtained by control of the duration of alkali hydrolysis. With the addition of mSF as a reinforcement in CS matrix, high-performance blended membranes were fabricated, especially for significantly increased mechanical properties. CS/mSF blended membranes also presented suitable swelling ratio and WVRT that are essential for an ideal wound dressing material. The result of *in vitro* cell experiment indicated that CS/mSF blended membranes presented good cytocompatibility. Silk microfibers embedded in CS matrix showed improved repair efficiency for full-thickness wound *in vivo* from both macroscopy and microscopy aspects. In conclusion, our results demonstrated blended membrane with CS and SF microfibers would be a promising candidate for use as a wound dressing.

4.Experimental Section

4.1 Materials

Silk cocoons of the silkworm *Bombyx mori.* were provided by the Institute of Huzhou Cocoon

Testing(PR China). Chitosan(degreeofdeacetylation: 90%-95%) was purchased from Shanghai Sangon Biotech Co., Ltd. Mouse fibroblast-like cells(L929) were purchased from Shanghai Institutes for Biological Sciences, Chinese Academy of Sciences. Fetal bovine serum(FBS), trypsinase, high-glucose Dulbecco's Modified Eagle's Medium(DMEM), penicillin, and streptomycin were purchased from GIBCO. The phosphate buffered saline(PBS) solution were purchased from Jinuo Biopharma Technology Co., Ltd. Sprague-Dawley rats were purchased from Zhejiang Province Laboratory Animal Center. The hematoxylin was purchased from SIGMA, and eosin was from Shanghai Maikun Chemical Co.,Ltd. All reagents were of analytical grade and were used as received without any further purification.

4.2 Preparation of silk microfibers(mSF)

mSF were prepared as described by previous report with some modifications.[27] Briefly, 10g cut pieces of silk cocoons were boiled for 30 minutes in 1000ml 0.5w/t% Na_2CO_3 solution to degum and rinsed throughly with deionized water, this degumming process was repeated once and then air dried. To obtain silk microfibers of different length, we immersed degummed silk into 1mol/L NaOH solution for 6, 12 and 24 hours under room temperature. The alkaline hydrolysis was stopped by excessive deionized water and the silk microfibers were washed for 5 times to remove NaOH residual. Dried mSF from wet silk slurry were prepared using hot air drier.

4.3 Preparation of CS/mSF blended membranes

2%(w/v) CS solution was first prepared by dissolving CS in 0.3mol/L acetic acid. Then mSF were added into CS solution, and mixed using magnetic stirring for 10 minutes to get homogeneous composite solution. The mass ratios of mSF to CS were stipulated as 0, 40, 60, and 80wt%. Pure CS membrane and CS/mSF blended membranes were developed by evaporation overnight at room

temperature from above solution. Then themembranes were immersed into 0.1mol/L NaOH methanol solution for 6 hours to insolubilize, and finally membranes were washed with deionized water to remove residue of methanol.

4.4 Characterization of pure CS membrane and CS/mSF blended membranes

4.4.1 Scanning electronic microscope(SEM)

Scanning electronic microscope(XL30-ESEM, Philip, The Netherlands) with an accelerating voltage of 20kV was used to observe the morphology of mSF and membrane samples. Before observing all samples were in totally dry state and sputtered with gold ion.

4.4.2 Mechanical properties

Membrane samples were cut into 50×8mm^2 strips and soaked in deionized water for 2 hours to balance prior to test. Universal tester(AGS-J, Shimadzu, Japan) equipped with a 50N capacity load cell was utilized to measure mechanical properties of wet membranes. All the tests were controlled by model at a speed of 3mm/min. The data of elastic modulus, tensile strength and elongation at break were reported from the stress-strain curves with means±SD (n=6).

4.4.3 Thermogravimetric analysis(TGA)

TGA instrument(DTG-60A, Shimadzu, Japan) was used for the thermogravimetric analysis of membranes. The tests were performed under nitrogen atmosphere (50ml/min) and the temperature was heated from 50 to 550℃ with a ramp rate of 10℃/min. The results were obtained by the software OriginPro 8.5.

4.4.4 Differential scanning calorimetry(DSC)

The thermal behaviors of membrane samples were detected using a DSC analyzer(822e, Mettler Toledo, Switzerland) under a nitrogen gas flow rate of 80ml/min. Test temperature range from 150

to 550℃ at heating rate of 10℃/min.

4.4.5 Swelling ratio

The swelling ratio was tested following the reported method.[49] Membrane samples were cut into 30×30mm^2 pieces and immersed into deionized water overnight. The wet weight of piece (W_s) was obtained after removing the excess water on the surface. The samples were dried in an oven at 50℃ for 6 hours and dried weight of piece was weighed (W_d). The swelling ratio (g/g) was calculated by following formula:

Swelling ratio=(W_s- W_d)/ W_d

The result was performed using means±SD (n=6).

4.4.6 Water Vapor Transmission Rate(WVTR) assay

WVTR assay was followed by our previous report.[50] Briefly, tested membranes were fixed on the opening of bottle (14 mm diameter) containing 10 ml deionized water. The initial weight of bottle was W_1(g). Then bottle was placed into an incubator with 39±2% relative humidity and 38±0.5℃ for 4 days. Afterward the bottle was weighed as W_2(g). Open bottle acted as blank group. WVTR of membrane was then calculated by following formula:

Q=(W_1- W_2)/ 4S

where Q represented WVTR(g/m^2 per 24h). S is the opening area of bottle(m^2). The result was performed using means±SD (n=6).

4.5 In vitro cell experiment

Cell proliferation on the membranes was detected using mouse fibroblast-like cells(L929) by 3-(4,5-dimethylthiazol-2-yl)-5-(3-carboxymethoxyphenyl)-2-(4-sulfophenyl)-2H-tetrazolium(MTS) assay. Pure CS membranes and blended CS/mSF membranes were cut into circular pieces with

diameters of 6.4mm, which then sterilized with 70% ethanol and UV irradiation. Sterilized membrane samples were placed into 96-well plates, then 200μl of cell suspension containing 5×10^3 cells was seeded onto each membrane. Cells and membranes complexes were incubated at 37℃ in a humidified atmosphere of 5% CO_2 for 1 and 3 days. The cell culture medium with 10% FBS, 100U/ml penicillin and 100μg/ml streptomycin was refreshed every 2 days. At the appointed time, cell proliferation was evaluated using MTS kit(Promega, USA) according to the manufacturer's protocol. Briefly, 100μl cell culture medium was removed, and 20μl MTS reagent was added to each well and plates were incubated at 37℃ for 4 hours. The optical density(OD) of each sample was detected at 490nm using a microplate reader(PLUS 384, Molecular Device, USA).

SEM was utilized to observe morphology of cells onto membranes. Before SEM measurement, seeded membranes were fixed with 2.5% glutaraldehyde and 2.5% osmic acidin PBS solution for 3 hours each at 4℃. The fixed membranes were dehydrated in increasing concentration of ethanol (30, 50, 70, 85, 95 and 100%) for 20 minutes each, then critically point dried. The dried samples were coated with gold ion by sputtering and observed using SEM(S-3000N, Hitachi, Japan).

4.6 In vivo wound healing study

4.6.1 Full-thickness skin wound model of rats

Healthy Sprague-Dawley rats(male, weighing 200 to 220g) were used to form full-thickness skin wound models. In detail, the surgical areas were shaved with an electric razor one day before operation. After anesthesia with an intraperitoneal injection of 10% chloral hydrate(3.5ml/kg body weight), the operation site of back skin centered on the spine was cleaned with 70% ethanol and iodine. Then acircular full-thickness wound of 2cm in diameter was madereferring toa template

line and the tissue excised to the layer of panniculus carnosus. The 45 treated rats were divided randomly into three groups, corresponding to control group, pure CS membrane group and 80% CS/mSF blended membrane group, respectively. The wounds of control group were smeared with vaseline cream, while the experiment groups were covered with CS pure membrane and 80% CS/mSF blended membrane. In addition, above the membranes sterilized gauze was sewed around skin to prevent the dressings from falling off. We confirm that all animal experiments in our study were carried out in accordance with the guidelines and approval(ZJU2015-474-02) of the Laboratory Animal Welfare Ethic Committee of Zhejiang University.

4.6.2 Measurement of wound size percentage

The wound region was photographed with a measuring scale at 7, 14 and 21 days using a digital camera(Canon IXUS610, Japan), and in each group 5 rats were measured at a time point. The wound area was measured by software MapInfo Professional 10.0, then the wound size was calculated compared to the initial state. The result was performed using means±SD (n=5).

4.6.3 Histological evaluation

The regenerated tissue at the wounds together with the surrounding uninjured skin was excised at 7, 14 and 21 days, as well as normal skin, were fixed in 10% phosphate-buffered formalin, and then embedded in a paraffin block. Sections of 4μm thickness were prepared by rotary microtome (RM2135, Leica, Germany) and stained with hematoxyline and eosin(H&E) reagents according to routine procedures. Histological changes were observed using microscope(BH2, Olympus, Japan).

4.7 Statistical analysis

All data were performed using means±SD of n=5-6. Statistical analyses were carried out using Software of SPSS 16.0. Statistically differences (*$p<0.05$,**$p<0.01$ or #$p<0.05$) were determined

by one-way ANOVA with a Student's T-Test.

Notes

† These authors contributed equally to this work.

Acknowledgments

This study is supported by the earmarked fund(CARS-22-ZJ0402) for China Agriculture Research System(CARS) and National Natural Science Foundation of China(21172194). We would like to thank Yu Zhu for revision of the manuscript.

References

1 R. Fu, C. Li, C. Yu, H. Xie, S. Shi, Z. Li, Q. Wang and L. Lu. *Drug*. *deliv*., 2014, 1-12.

2 A. Vasconcelos, A.C. Gomes and A. Cavaco-Paulo. *Acta*. *Biomater*., 2012, **8**, 3049-3060.

3 Z. Gu, H. Xie, C. Huang, L. Li and X. Yu. *Int*. *J*. *Biol*. *Macromol*., 2013, **58**, 121-126.

4 R. Jayakumar, D. Menon, K. Manzoor, S. Nair and H. Tamura. *Carbohydr*. *Polym*., 2010, **82**, 227-232.

5 I. Y. Kim, S. J. Seo, H. S. Moon, M. K. Yoo, I. Y. Park, B. C. Kim and C. S. Cho. *Biotechnol*. *Adv*., 2008, **26**, 1-21.

6 S. K. L. Levengood and M. Zhang. *J*. *Mater*. *Chem*. *B*, 2014, **2**, 3161-3184.

7 D. Archana, J. Dutta and P. Dutta. *Int*. *J*. *Biol*. *Macromol*., 2013, **57**, 193-203.

8 D. Archana, B. K. Singh, J. Dutta and P. Dutta. *Carbohydr*. *Polym*., 2013, **95**, 530-539.

9 M. Y. Bai, T. C. Chou, J. C. Tsai and W. C. Yu. *J*. *Biomed*. *Mater*. *Res*., *Part A*, 2014, **102**, 2324-2333.

10 E. Lih, J. S. Lee, K. M. Park and K. D. Park. *Acta*. *Biomater*., 2012, **8**, 3261-3269.

11 A. Hashemi Doulabi, H, Mirzadeh, M. Imani and N. Samadi. *Carbohydr*. *Polym*., 2013, **92**, 48-56.

12 H. F. Shi, X. G. Wang, S. C. Wu, Z. W. Mao, C. G. You and C. M. Han. *J*. *Mech*. *Beha*. *Biomed*. *Mater*., 2014, **29**, 114-125.

13 Y. Cao and B. Wang. *Int*. *J*. *Mol*. *Sci*., 2009, **10**, 1514-1524.

14 Z. Shao and F. Vollrath. *Nature*, 2002, **418**, 741.

15 B. D. Lawrence, J. K. Marchant, M. A. Pindrus, F. G. Omenetto and D. L. Kaplan. *Biomaterials*., 2009, **30**, 1299-1308.

16 B. Kundu, R. Rajkhowa, S. C. Kundu and X. Wang. *Adv*. *Drug Delivery Rev*., 2013, **65**, 457-470.

17 E. M. Pritchard and D. L. Kaplan. *Expert*. *Opin*. *Drug*. *Deliv*., 2011, **8**, 797-811.

18 H. Lee, C. H. Jang and G. H. Kim. *J*. *Mater*. *Chem*. *B*, 2014, **2**, 2703-2713.

19 A. R. Murphy and D.L. Kaplan. *J*. *Mater*. *Chem*., 2009, **19**, 6443-6450.

20 A. S. Mehta, B. K. Singh, N. Singh, D. Archana, K. Snigdha, R. Harniman, S. S. Rahatekar and R. Tewair, P. Dutta. *J*. *Biomater*. *Appl*., 2014, 0885328214563148.

21 D. H. Roh, S. Y. Kang, J. Y. Kim, Y. B. Kwon, H. Young Kweon, K.G. Lee, Y. H. Park, R. M. Baek, C. Y. Heo, J. Choe and J. H. Lee. *J*. *Mater*. *Sci*. *Mater*. *Med*., 2006, **17**, 547-552.

22 R. Okabayashi, M. Nakamura, T. Okabayashi, Y. Tanaka, A. Nagai and K. Yamashita. *J*. *Biomed*. *Mater*. *Res*. *B*. *Appl*. *Biomater*. 2009, **90**, 641-646.

23 Z. Karahaliloglu, B. Ercan, E. B. Denkbas and T. J. Webster. *J*. *Biomed*. *Mater*. *Res*., *Part A*, 2015, **103**, 135-144.

24 W. Luangbudnark, J. Viyoch, W. Laupattarakasem, P. Surakunprapha and P. Laupattarakasem. *ScientificWorldJournal*., 2012, **2012**, 697201.

25 Z. X. Cai, X. M. Mo, K. H. Zhang, L. P. Fan, A. L. Yin, C. L. He and H. S. Wang. *Int. J. Mol . Sci*., 2010, **11**, 3529-3539.

26 K. H. Zhang, Q. Z. Yu and X. M. Mo. *Int. J. Mol. Sci*., 2011, **12**, 2187-2199.

27 B. B. Mandal, A. Grinberg, E. S. Gil, B. Panilaitis and D. L. Kaplan. *Pro. Natl. Acad. Sci. USA*., 2012, **109**, 7699-7704.

28 S. Yodmuang, S. L. McNamara, A. B. Nover, B. B. Mandal, M. Agarwal, T. A. Kelly, P. H. Chao, C. Hung, D. L. Kaplan and G. Vunjak-Novakovic. *Acta. Biomater*., 2015, **11**, 27-36.

29 S. Mobini, B. Hoyer, M. Solati-Hashjin, A. Lode, N. Nosoudi, A. Samadikuchaksaraei and M. Gelinsky. *J. Biomed. Mater. Res*., *Part A*, 2013, **101**, 2392-2404.

30 S. D. McCullen, C. M. Haslauer and E. G. Loboa. *J. Mater. Chem*., 2010, **20**, 8776-8788.

31 B. K. Gu, S. J. Park, M. S. Kim, C. M. Kang, J. I. Kim and C. H. Kim. *Carbohydr. Polym*., 2013, **97**, 65-73.

32 S. F. Wang, L. Shen, W. D. Zhang and Y. J. Tong. *Biomacromolecules*., 2005, **6**, 3067-3072.

33 Q. Hu, B. Li, M. Wang and J. Shen. *Biomaterials*., 2004, **25**, 779-785.

34 L. S. Guinesi and É. T. G. Cavalheiro. *Thermochimica. Acta*., 2006, **444**, 128-133.

35 M. A. de Moraes and M. M. Beppu. *J. Appli. Polym. Sci*., 2013, **130**, 3451-3457.

36 C. Z. Zhou, F. Confalonieri, M. Jacquet, R. Perasso, Z. G Li and J. Janin. *Proteins*., 2001, **44**, 119-122.

37 N. L. Yusof, A. Wee, L. Y and Lim, E. Khor. *J. Biomed. Mater. Res*., *Part A*, 2003, **66**, 224-232.

38 B. D. Lawrence, Z. Pan and M. I. Rosenblatt. *PloS one*., 2012, **7**, e50190.

39 X. Hu, S. H. Park, E. S. Gil, X. X. Xia, A. S. Weiss and D. L. Kaplan. *Biomaterials*., 2011, **32**, 8979-8989.

40 D. E. Discher, P. Janmey and Y. L. Wang. *Science*., 2005, **310**, 1139-1143.

41 S. Kanokpanont, S. Damrongsakkul, J. Ratanavaraporn and P. Aramwit. *Int. J. Pharm*., 2012, **436**, 141-153.

42 E. S. Gil, B. Panilaitis, E. Bellas and D. L. Kaplan. *Adv. Healthc. Mater*., 2013, **2**, 206-217.

43 R. F. Diegelmann and M. C. Evans. *Front. Biosci*., 2004, **9**, 283-289.

44 G. H. Altman, F. Diaz, C. Jakuba, T. Calabro, R. L. Horan, J. Chen, H. Lu, J. Richmond and D. L. Kaplan. *Biomaterials*., 2003, **24**, 401-416.

45 L. Meinel, S. Hofmann, V. Karageorgiou, C. Kirker-Head, J. McCool, G. Gronowicz, L. Zichner, R. Langer, G. Vunjak-Novakovic and D. L. Kaplan. *Biomaterials*., 2005, **26**, 147-155.

46 R. Jayakumar, M. Prabaharan, P. T. Sudheesh Kumar, S. V. Nair and H. Tamura. *Biotechnol. Adv*., 2011, **29**, 322-337.

47 A. Sugihara, K. Sugiura, H. Morita, T. Ninagawa, K. Tubouchi, R. Tobe, M. Izumiya, T. Horio, N. G. Abraham and S. Ikehara. *Proc. Soc. Exp Bio. Med*., 2000, **225**, 58-64.

48 K. Zhang, Y. Qian, H. Wang, L. Fan, C. Huang, A. Yin and X. Mo. *J. Biomed. Mater. Res*., *Part A*, 2010, **95**, 870-881.

49 S. Yan, Q. Zhang, J. Wang, Y. Liu, S. Lu, M. Li and D. L. Kaplan. *Acta. Biomater*., 2013, **9**, 6771-6782.

50 S. Min, X. Gao, C Han, Y. Chen, M. Yang, L. Zhu, H. Zhang, L. Liu and J. Yao. *J. Biomater. Sci. Polym. Ed*., 2012, **23**, 97-110.

Captions to figures

Fig.1 Silk microfibers with different length after alkali hydrolyzing for (**A**)6 hours; (**B**)12 hours; and (**C**)24 hours. (Scale bar, 100μm).

Fig.2 Photographs(left) and SEM images(right) of membranes. (Scar bars, 3cm and 100μm).

Fig.3 Mechanical properties of membranes in wet condition. (**A**)Stress-strain curves; (**B**)Elastic Modulus; (**C**)Tensile strength; (**D**)Elongation at break.

Fig.4 (A) TGA thermographs curves and **(B)** DSC curves of membranes.

Fig.5(A) Swelling ratio and **(B)**Water vapor transmission rate of membranes. Asterisk (*) and (**) mean the statistically difference compared to pure CS membrane, $^{*}p<0.05$ and $^{**}p<0.01$, n=6.

Fig.6 (A) Proliferation of L929 cells on tested membranes for 1 and 3 days. Asterisk(*) means statistically difference compared to pure CS membrane, $^{*}p<0.05$, n=4. **(B)** SEM images of L929 cells cultured onto membranes for 1 and 3 days.(Scale bar, 200μm).

Fig.7(A) Photographs of macroscopical wound condition, black scale bar, 0.5cm. **(B)** Percentage of wound size compared with initial one at 0 day, Asterisk (**) means statistically difference compared to Control and (#) means statistically difference compared to CS, $^{**}p<0.01$, $^{\#}p<0.05$, n=5. Control(covered with vaseline cream); Pure CS(pure CS membrane); CS/mSF(80% CS/mSF blended membrane).

Fig.8 Histological photographs of wound sections stained with H&E.

IC: Inflammatory cells; **GT:** Granulation tissue; **F:** Fibroblasts; **K:**Keratinocytes; **NBV:** New blood vessels; **CF:** Collagen fiber; **NE:** New epithelium; **HFC:** Hair follicle cells.

Control(covered with vaseline cream); CS(pure CS membrane); CS/mSF(80%CS/mSF blended membrane).

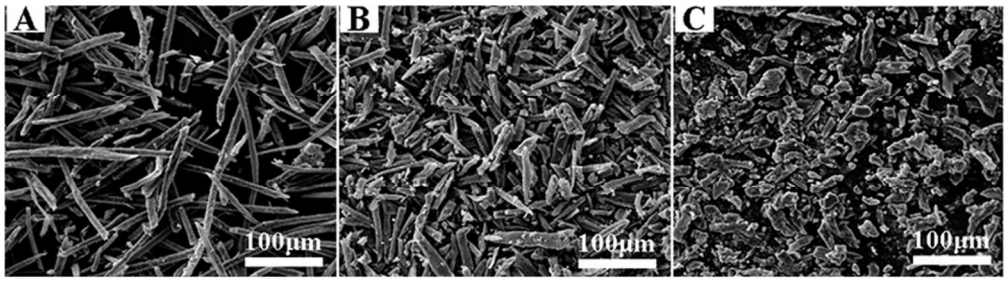

294x80mm (72 x 72 DPI)

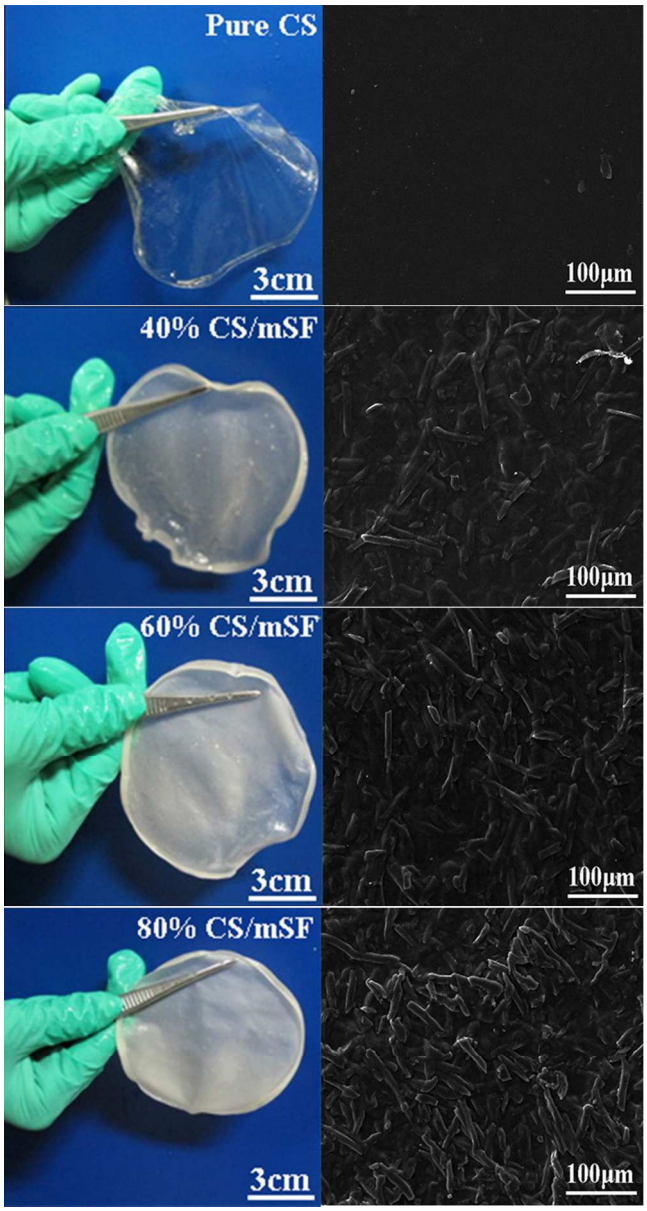

249x469mm (72 x 72 DPI)

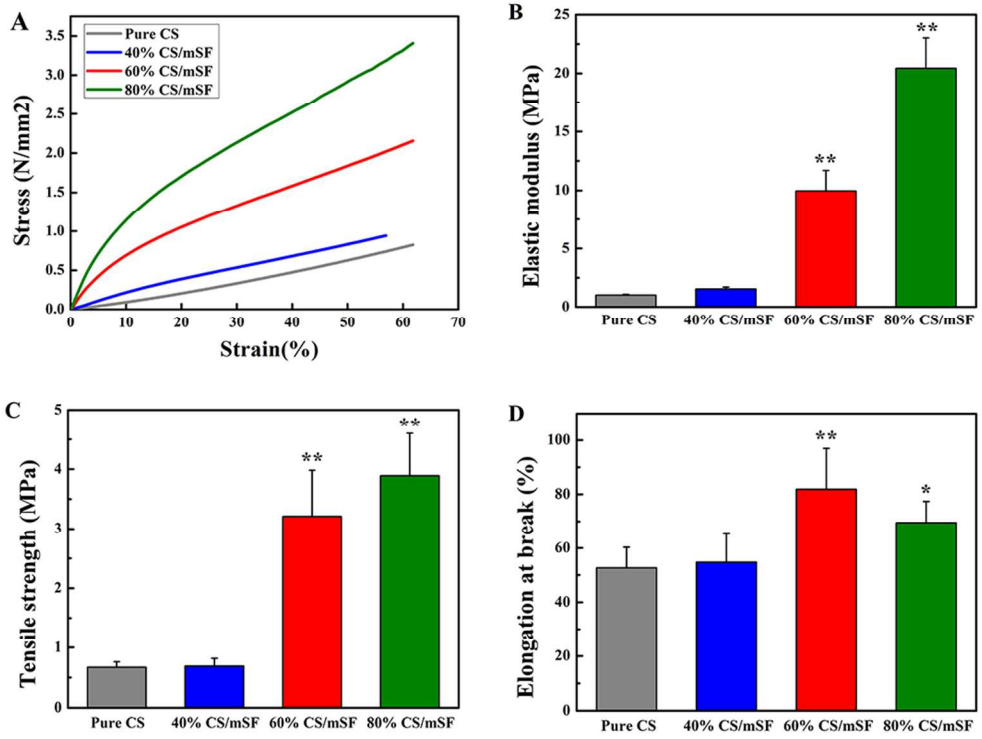

383x287mm (72 x 72 DPI)

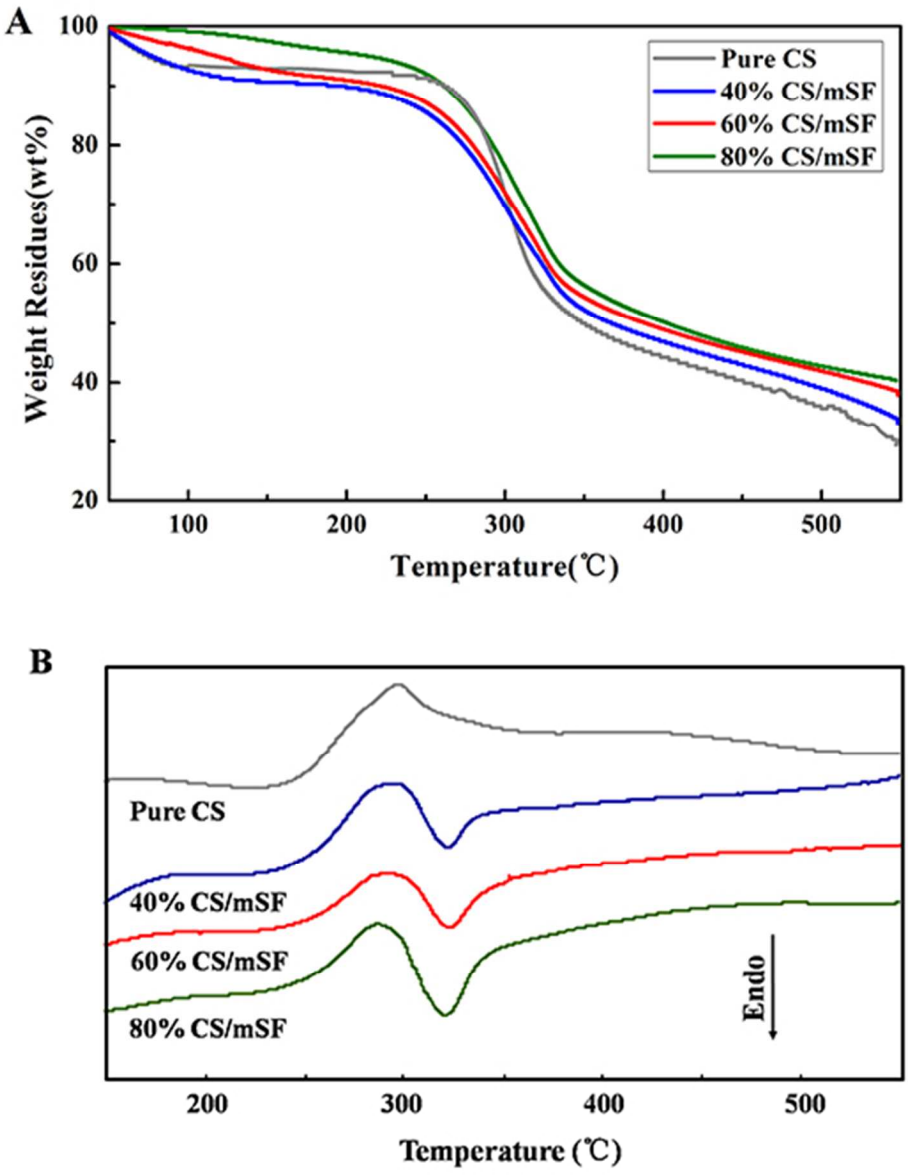

190x239mm (72 x 72 DPI)

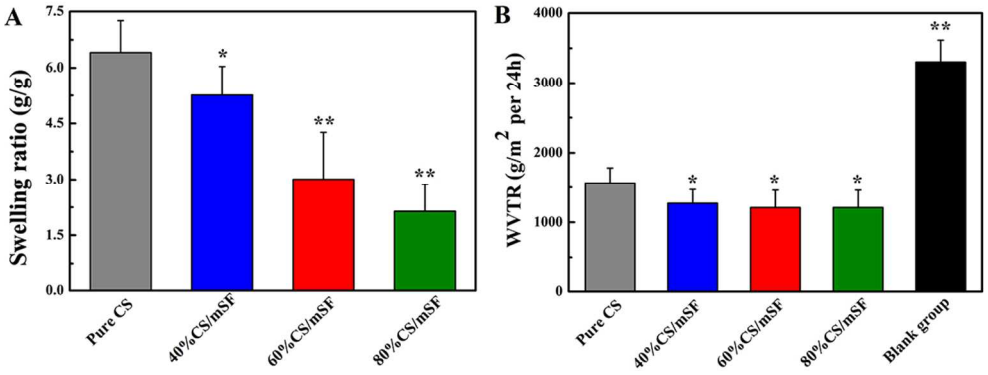

430x170mm (72 x 72 DPI)

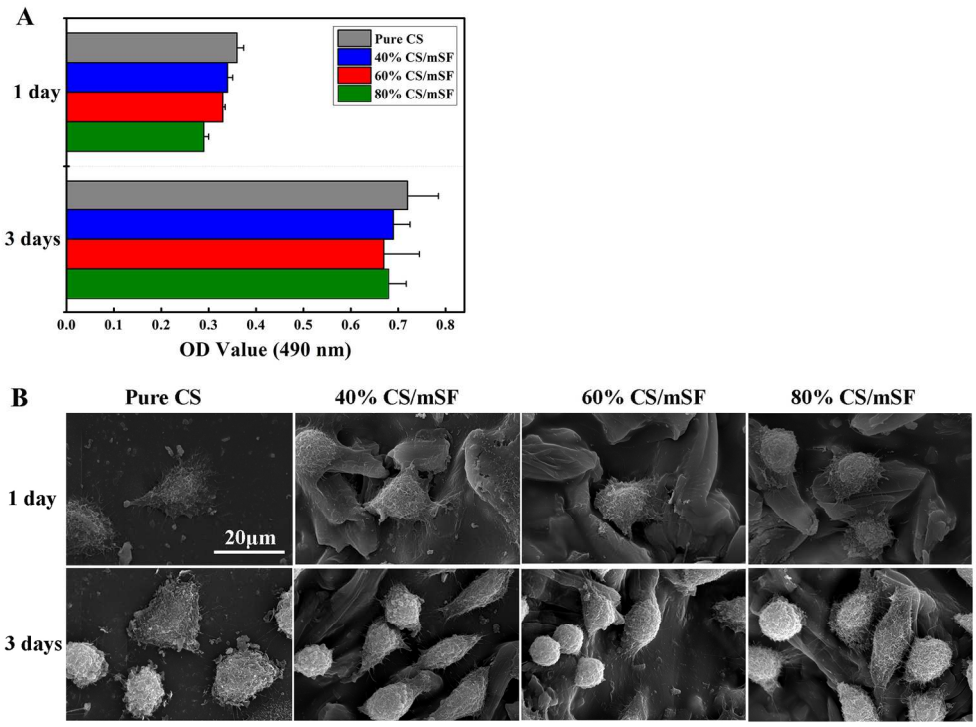

720x529mm (72 x 72 DPI)

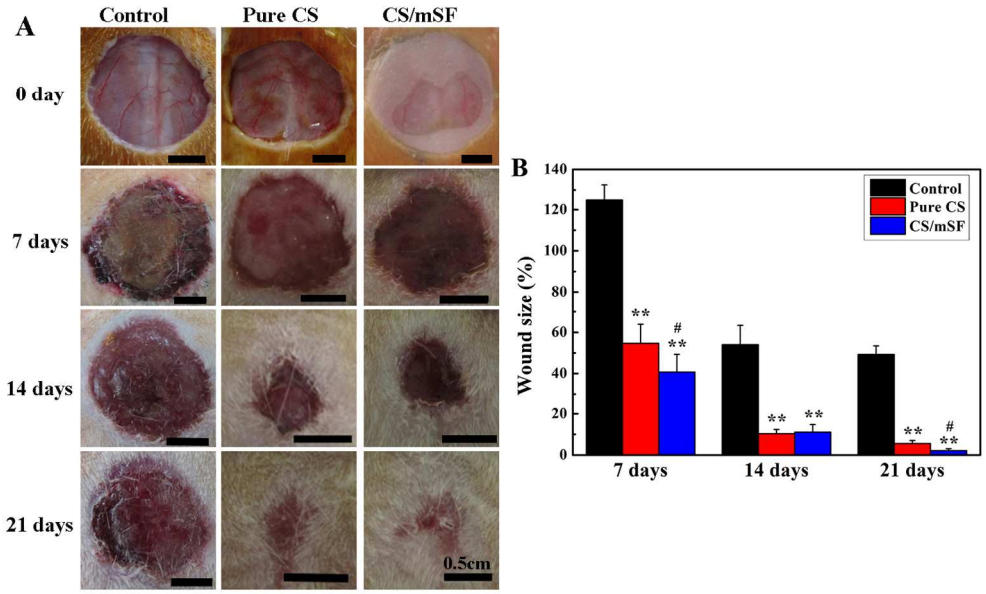

600x370mm (72 x 72 DPI)

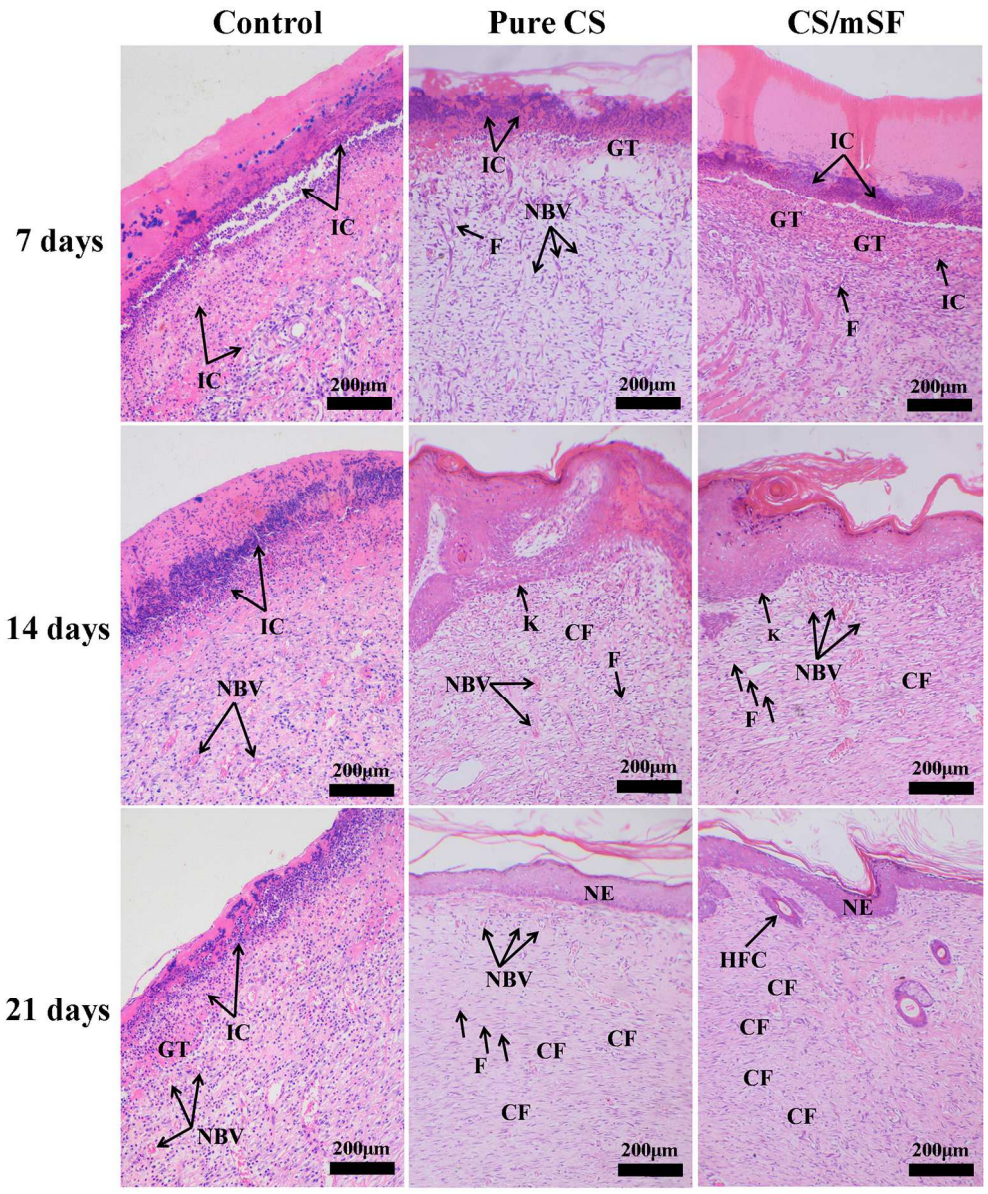

639x770mm (72 x 72 DPI)

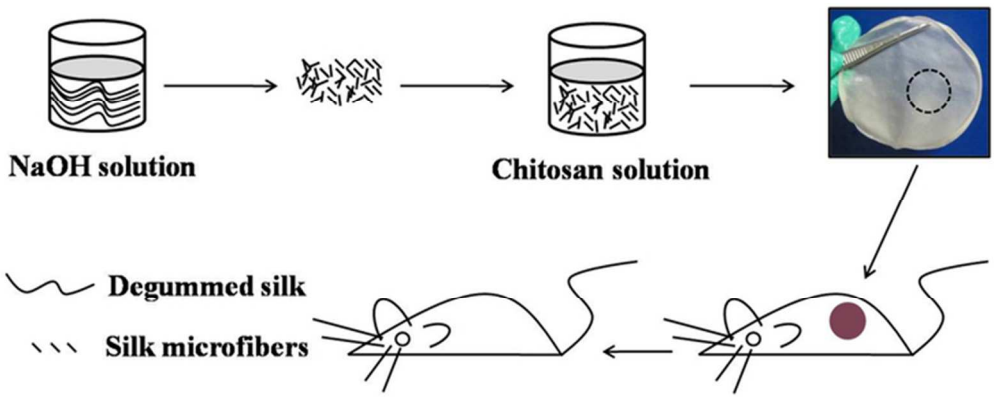

A novel type of chitosan/silk microfibers blended membrane were fabricated, which could significantly accelerate wound healing efficiency.
30x12mm (600 x 600 DPI)